Available online at www.sciencedirect.com
SCIENCE DIRECT®
Journal of Solid State Chemistry 177 (2004) 3879–3885
JOURNAL OF SOLID STATE CHEMISTRY
www.elsevier.com/locate/jssc

Origin of photoluminescence in $SrTiO_3$: a combined experimental and theoretical study

Emmanuelle Orhan[a,*], Fenelon M. Pontes[b], Carlos D. Pinheiro[b,e], Tania M. Boschi[c], Edson R. Leite[b], Paulo S. Pizani[c], Armando Beltrán[d], Juan Andrés[d], José A. Varela[a], Elson Longo[b]

[a]*Instituto de Química - Universidade Estadual Paulista, Araraquara, 14801-907 SP, Brazil*
[b]*Departamento de Química, Universidade Federal de São Carlos, São Carlos 13565-905 SP, Brazil*
[c]*Departamento de Física, Universidade Federal de São Carlos, Caixa Postal 676, São Carlos, 13565-905 SP, Brazil*
[d]*Departament de Ciències Experimentals, Universitat Jaume I, PO Box 6029, AP 12080 Castelló, Spain*
[e]*DCEN/CFP/UFPB, Cajazeiras, PB, Brazil*

Received 29 January 2004; received in revised form 19 July 2004; accepted 21 July 2004
Available online 21 September 2004

Abstract

A joint experimental and theoretical study has been carried out to rationalize the photoluminescence properties of $SrTiO_3$ perovskite thin films synthesized through a soft chemical processing. Only the amorphous samples present photoluminescence at room temperature. From the theoretical side, first principles quantum mechanical techniques, based on density functional theory at B3LYP level, have been employed to study the electronic structure of a crystalline (ST-c) and an asymmetric (ST-a) model. Electronic properties are analyzed in the light of the experimental results and their relevance in relation to the PL behavior of ST is discussed.

Keywords: Perovskite; Thin films; Photoluminescence; DFT; Electronic structure; Interplay theory experiment; $SrTiO_3$; Periodic calculation

1. Introduction

There is much interest in the areas of science and technology in transition metal oxides with an ABO_3 perovskite structure, owing to their wide variety of unique electronic, magnetic and optical properties [1–7]. Within this class of compounds, $SrTiO_3$ (ST), in its crystalline form, displays a semiconductor behavior and when pure ST is excited by radiation above its energy band gap, which usually ranges from 3.2 to 3.4 eV when optically determined [8–12], a broad luminescent band appears at low temperatures [13–15]. In this paper, we show the intense visible PL spectra of amorphous ST thin films measured at room temperature. Since there, the study of PL behavior in disordered or nanostructured materials [16] had focused on the development of new electroluminescent materials, owing to their potential technological applications, which include flat-screen full-color displays. Our group already published numerous experimental studies on amorphous perovskite titanates $ATiO_3$ where A = Pb, Ca, Sr and Ba [17–25].

However, despite intense experimental efforts, a clear understanding of the PL behavior of ST and related ABO_3 materials has yet to emerge. Some authors propose a mechanism involving self-trapped excitons (STE) [13], others show through semi-empirical quantum chemical calculations that the origin of the intrinsic excitonic (“green”) luminescence of ABO_3 perovskites at low temperature would be linked to the recombination of electrons and hole polarons forming a charge transfer vibronic exciton (CTVE) [26].

*Corresponding author. Fax: +55-16-3360-8350.
E-mail address: emmanuelle.orhan@liec.ufscar.br (E. Orhan).

0022-4596/$ - see front matter © 2004 Elsevier Inc. All rights reserved.
doi:10.1016/j.jssc.2004.07.043

What remains unclear are the rules allowing PL emission in the visible range in relation to temperature and lattice geometry. Bouma and Blasse [27] concluded from their extended experimental studies on titanates that compounds involving an irregular titanate octahedron with a short Ti–O distance show PL at room temperature, if these octahedra are isolated from each other. They ascribed this effect to a broadening of the energy bands.

In the past, we performed combined experimental and semi-empirical theoretical studies on clusters for trying to understand the relations between crystalline structure and PL [28–32]. In the present work, high level first principles calculations in the frame of density functional theory at B3LYP level are used, associated with new results on crystalline and amorphous ST thin films, into a synergetic strategy for understanding the PL behavior of ST. But, like Canadell et al. [33] say, being able to calculate does not mean being able to understand in simple terms. It is of first importance for a good interplay between theoretical and experimental works to use simple but yet rigorous frame work, following the pioneering ideas of Hoffman, Burdett and Whangbo [34–36] who built a bridge between the concepts developed by solid state physicists and molecular chemists. The aim of the theoretical part is to investigate the electronic structure of ST by means of simple periodic models and to give a microscopic interpretation of the PL properties of this system in terms of density of states (DOS), band structure diagrams and electronic charge densities. The experimental work presents measurements of broad, intense visible PL at room temperature in ST amorphous thin films prepared at low temperatures by the polymeric precursor method [21,37]. This approach renders a plausible quantitative description of the PL of ST and an interesting correlation between the theoretical and experimental results.

The layout of the paper is as follows: first section contains the experimental details of the techniques used for the synthesis and characterization of the thin film samples. The computational methods are detailed in the second one. Third section presents the perovskite crystal structure and the periodic models selected to represent the crystalline and amorphous thin films. An analyze and discussion of the results is given in the next section and finally, the last one collects our conclusions.

2. Experimental

ST thin films studied in the present work were derived from a soft chemical processing. Details of the preparation method can be found in the literature [21,37]. The heat treatment was carried out at 573 K in a tube furnace under oxygen flow, at a heating rate of 5 K/min, for 32 h to pyrolyse the organic materials. The ST thin films were structurally characterized using X-ray diffraction (XRD) (Cu$K\alpha$ radiation). The diffraction patterns were recorded on a Siemens D5000 machine in a $\theta-2\theta$ configuration, using a graphite monochromator. The spectral dependence of optical absorbance for the crystalline and amorphous ST on quartz substrates were taken at room temperature in the total reflection mode, using a Cary 5G equipment. The PL spectra of the ST thin films were taken with a U1000 Jobin-Yvon double monochromator coupled to a cooled GaAs photomultiplier and a conventional photon counting system. The 457.9, 488.0, and 514.5 nm exciting wavelengths of an argon ion laser was used, with the laser's maximum output power kept at 20 mW. A cylindrical lens was used to prevent the sample from overheating. The slit width used was 100 μm. The measurements were taken at room temperature and at 10 K.

3. Computational details

Calculations have been carried out with the CRYSTAL98 [38] package within the framework of the density functional theory using the gradient-corrected correlation functional by Lee, Yang and Parr, combined with the Becke3 exchange functional, B3LYP [39,40], which has been demonstrated by Muscat et al. [41] to be suitable for calculating structural parameters and band structures for a wide variety of solids. The atomic centers have been described by all electron basis sets 976-41(d51)G for Sr [42], 86-411(d31)G for Ti and 6-31G* for O [43]. The k-points sampling was chosen to be 40 points within the irreducible part of the Brillouin zone. For simulating the displacement of the Ti atom, as explained in the next section, we have used the ATOMDISP option provided with the CRYSTAL program. The XCrysDen program was used to design the DOS and the band structure diagrams [44].

4. Crystal structure and periodic models

ST crystallizes in the cubic perovskite structure (space group $Pm3m$, O_h symmetry). The strontium atoms share the corners of the unit cell and the titanium is at the center of the cube, surrounded by six oxygens that occupy the middle of the faces, in a regular octahedral configuration. We have used a $1\times1\times2$ supercell as a periodic model for representing the crystalline ST (ST-c). It results in 10 atoms in the unit cell, see Fig. 1. This ST-c model can be designed as $[TiO_6]$–$[TiO_6]$, as each titanium is surrounded by 6 O in a O_h configuration.

The experimental and calculated values of **a** parameter are 3.90 and 3.88 Å, respectively.

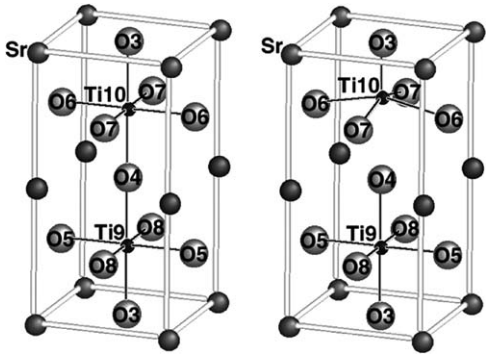

Fig. 1. Supercell $1 \times 1 \times 2$ of the cubic $SrTiO_3$ unit cell in the crystalline form, i.e., ST-c periodic model (left) and after displacement of Ti10, ST-a periodic model (right).

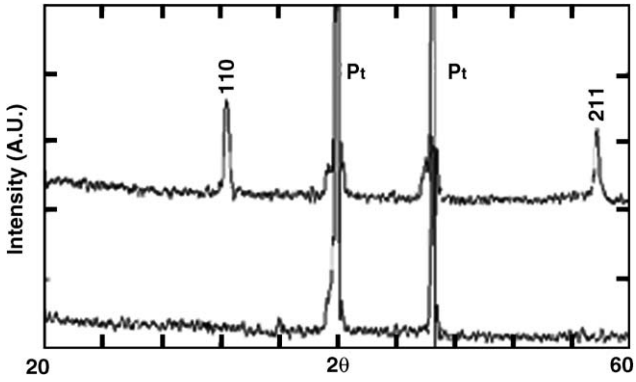

Fig. 2. DRX patterns of the crystalline (top) and amorphous (bottom) $SrTiO_3$ thin films on Pt substrate.

XANES experimental results [32] on the amorphous phase of ST pointed out the coexistence of two types of environments for the titanium, namely, fivefold titanium coordination ($[TiO_5]$ square-base pyramid) and sixfold titanium coordination ($[TiO_6]$ octahedron). This certain degree of order in amorphous materials was to be expected, since two or more atoms arranged close to each other in a stable configuration must necessarily have some degree of order because there always exist minima of the potential energy. Furthermore, as it is well known, the details of the band structure for a periodic system is mainly determined by the potential within the unit cell, rather than by the long range periodicity. This means that any symmetry perturbation in the unit cell will have heavy consequences on the electronic structure.

Based on these results, we model the ST amorphous phase by shifting the titanium 10 by a (0 0 0.5) Å vector from its previous position in the former $1 \times 1 \times 2$ supercell. This displacement asymmetries the unit cell, in which Ti10 is now surrounded by 5 oxygens in a square-base pyramid configuration while Ti9 surroundings remain 6 oxygens as in the ST-c case. Therefore, this asymmetric ST model, ST-a, represents the ST amorphous material. This structure can be designed as $[TiO_6]$–$[TiO_5]$, see Fig. 1. Our aim with this modelization is not to represent the exact reality of the amorphous phase, but to offer a simple scheme allowing to understand the effects of structural deformation on the electronic structure without completely suppressing the geometry of the cell that is useful for the periodic calculation.

5. Results and discussion

Fig. 2 shows the XRD patterns of two ST thin films prepared by the polymeric precursor method, deposited on platinum-coated silicon substrate and annealed in an oxygen flow at 973 K for 2 h for the first one and at 573 K for 32 h for the second one. The (110) and (211) diffraction peaks of the crystalline thin film are clearly distinguished from the Pt substrate peaks. For the second thin film, only the peaks related to the Pt substrate are appearing, attesting for structural disorder.

Fig. 3 shows the PL spectra measured at room temperature for the amorphous thin film (1), at room temperature (2) and at 10 K (3) for the crystalline thin film. Both thin films were excited with the 488 nm line of an argon ion laser. The amorphous thin film spectrum shows a strong PL while the crystalline thin film does not present any PL, neither at room temperature nor at 10 K, although some authors reported PL at 35 K for crystalline powders obtained from high temperature oxide mixing [45]. The PL of ST in the visible range essentially depends on its crystalline structure; it is linked to structural disorder. We think that our thin films preparation method offers a far lower defects concentration than a classical oxide mixing method, and therefore the crystalline thin films does not show PL at low temperatures.

When the amorphous thin film is excited by various laser lines (Fig. 4), it always presents a strong PL, with variations in the maximum emission wavelengths. Moreover, a linear relation between the maximum wavelength of emission peak and the exciting wavelength was observed (inset of Fig. 4). This results suggest that the emission can be tuned by the exciting wavelength, thus that the PL of the amorphous thin film occurs from a continuous excitation process.

In Fig. 5, the spectral dependence of the absorbance for the amorphous and crystalline ST thin films is presented. The crystalline thin film presents only one, well-defined, absorption front (linear part of the curve) while the amorphous thin film exhibits typically two absorption fronts with a tail at low energies, suggesting the presence of localized states inside the band gap. The optical gaps obtained by extrapolation of the linear curve regions are 3.5 eV for the crystalline thin film and 1.43 eV for the amorphous one. The value of the

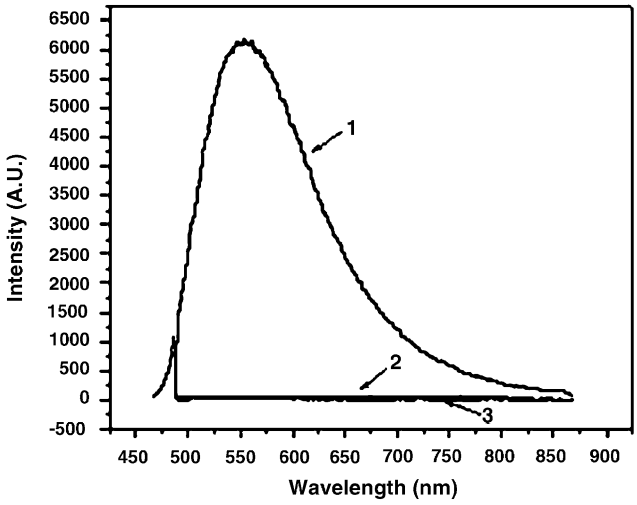

Fig. 3. Photoluminescence spectra of $SrTiO_3$ thin films: (1) amorphous at 300 K; (2) crystalline at 300 K and (3) crystalline 10 K. All thin films were excited with the 488 nm line of an argon ion laser.

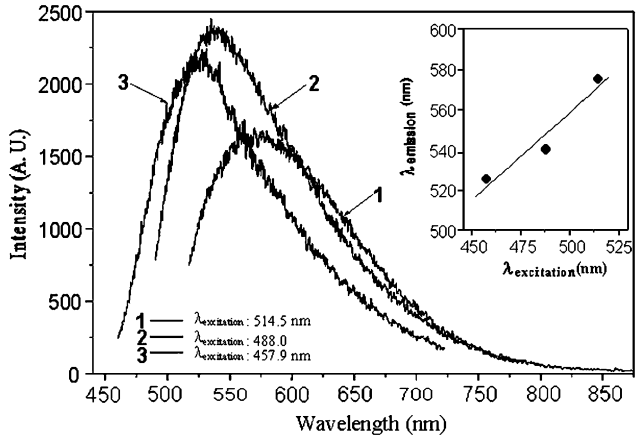

Fig. 4. Photoluminescence spectra of amorphous $SrTiO_3$ thin films as a function of exciting wavelength. The inset shows the emission peak wavelength as a function of exciting wavelength.

crystalline gap in Ref [17] was 3.73 eV. This difference may be due to the quantum size confinement effect [46].

The aforementioned experimental results strongly indicate that photoluminescence is directly related to the structural disorder and to the optical edges and tails. The nature of these optical edges and tails may be associated with defect states promoted by the disordered structure of the amorphous ST. The absorbance measurements, associated with the PL characterization of amorphous ST thin films, suggest a non-uniform band gap structure with a tail of localized states and mobile edges. As explained by Blasse [47], the PL arises from a radiative return to the ground state, phenomenon that is in concurrence with the non-radiative return to the ground state where the energy of the excited state

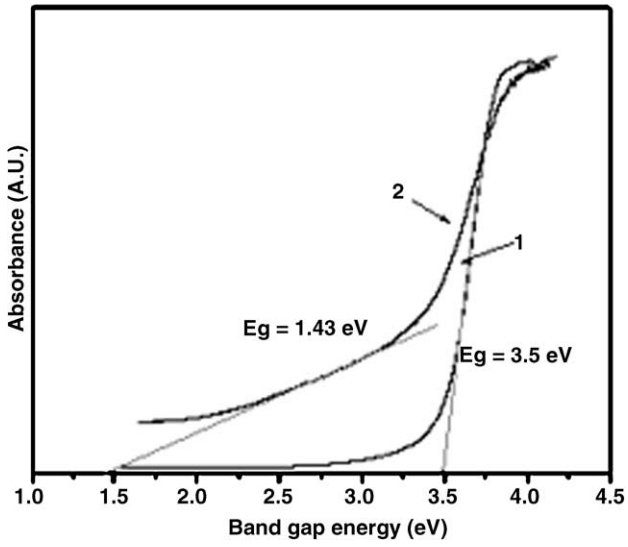

Fig. 5. Spectral dependence of the absorbance for the crystalline (1) and amorphous (2) and $SrTiO_3$ thin films. The numbers correspond to the values of the optical gaps.

is used to excite the vibrations of the host lattice, i.e., to heat the lattice. The radiative emission process occurs more easily if exist in the structure trapped holes or trapped electrons. In order to evidence the presence of trapped holes and trapped electrons in our amorphous thin film, we performed a detailed theoretical study of the electronic structure in a cubic, ST-c, and disordered (asymmetric) material, ST-a. To analyze the differences in the electronic structure, it is convenient to make reference to quantities such as the band gap or the projected densities of states (DOS) which may be compared to each other independently of the crystalline space group.

Fig. 6 (top) reports the calculated band structure of bulk ST-c. Top of the valence band (VB) is at M point and is very close to the X point. Bottom of conduction band (CB) is at Γ. The minimal indirect gap between M and Γ is 3.80 eV, very close to the experimental one deduced from the observed optical absorption edge, that we found to be 3.50 eV. The minimal direct gap at Γ is 4.02 eV.

The calculated band structure of bulk ST-a is depicted in Fig. 6 (bottom). The top of the VB is at M point and bottom of CB is at Γ, as in the case of ST-c. The indirect minimal gap between M and Γ is 2.90 eV while the minimal direct gap at Γ is 3.72 eV. The indirect gap can be compared with the optical gap of the amorphous thin film that we found to be 1.43 eV. These results show that our data are consistent with the interpretation that the exponential optical absorption edge and the optical band gap are controlled by the degree of disorder, structural and thermal, in the lattice of ST system (see Fig. 5).

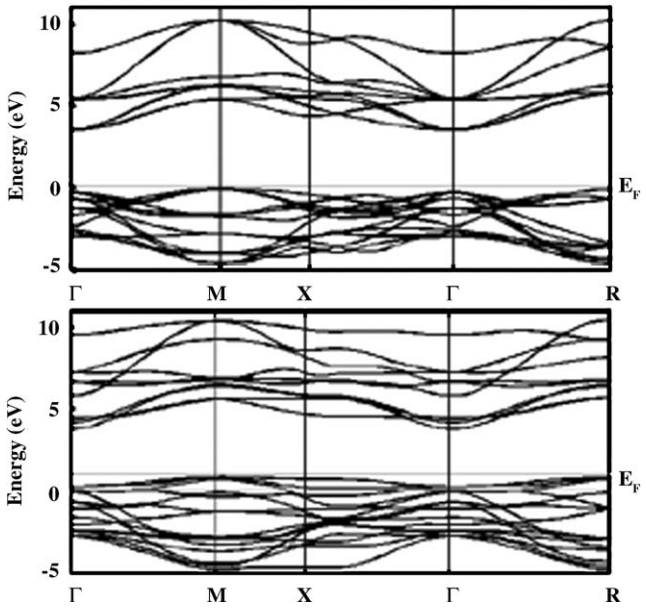

Fig. 6. Band structure for ST-c (top) and ST-a (bottom). The zero is taken at the top of the ST-c valence band.

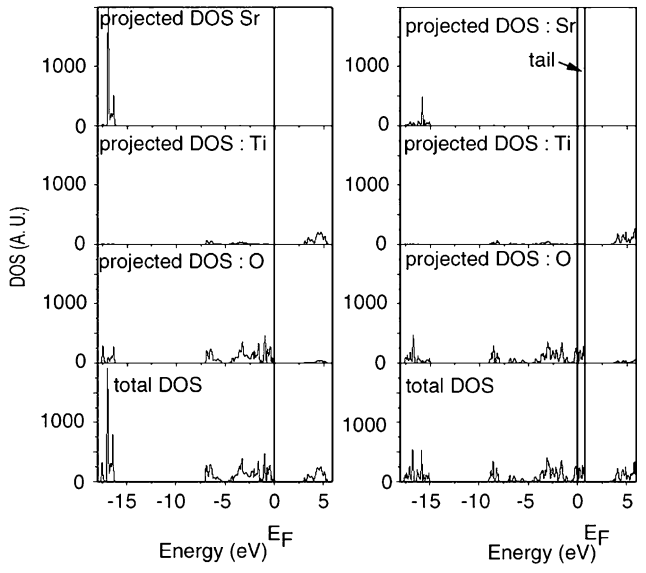

Fig. 7. Total and atom projected DOS for ST-c (left) and ST-a (right).

The calculated total and atom-resolved projected DOS of ST-c and ST-a models are shown in Fig. 7, ranging from −18 eV below the top of the VB to 6 eV above. In the case of ST-c, the upper VB is predominately made of the O (2*p*) states, equivalently distributed on the six oxygens of the structure. In the case of ST-a, although the VB is also made of the O (2*p*) states, the upper part, i.e., the new states, present a strong O4 character, the oxygen atom that looses the connection with Ti10. The CB is clearly made of the Ti (3*d*) states in both cases. The Ti–O covalent bond creates a limited Ti (3*d*) contribution in the O (2*p*) region as well as a weak O (2*p*) contribution to the Ti (3*d*) area. The Sr (5*s*) states (not shown) are to be found between –16 and –17 eV in the case of ST-c and, more dispersed, between –15 and –18 eV in the case of ST-a. These levels are weakly hybridized with the oxygen levels.

It is also interesting to complement the present results with the analysis of the contour and surface plots of the electronic charge density calculated on a selected plane for ST-c and ST-a structures, respectively in Figs. 8a and b. The chosen plane is a vertical diagonal plane containing the Sr1, Sr2, Ti9, Ti10, O3 and O4 atoms. It is shown by the gray areas in the cell representations. The charge densities are calculated from a Mulliken analysis that is relevant enough in a comparison purpose between two models. An analysis of the Fig. 8 clearly shows that the bonding between Sr and [TiO_6] is strongly ionic, while a covalent bonding nature is visible between Ti and O result of the hybridization between the O (2*p*) states and the Ti (3*d*) states. The breaking of the Ti10–O4 bond is visible in Fig. 8b. The displacement of a metallic center on going from ST-c to ST-a results in the deformation of a symmetric [TiO_6–TiO_6] structure into two fragments: [TiO_6] and [TiO_5]. The formal net charges indicated on the crystal cell show that, as expected, the symmetric [TiO_6–TiO_6] possesses a regular charge repartition on both [TiO_6] clusters, −1.98*e* and 3.97*e* on the complete Sr network. In the case of the deformed structure (right margin of Fig. 8), the formal charges of the [TiO_6] and [TiO_5] clusters become, respectively, –2.69*e* and –1.28*e*, and the Sr network

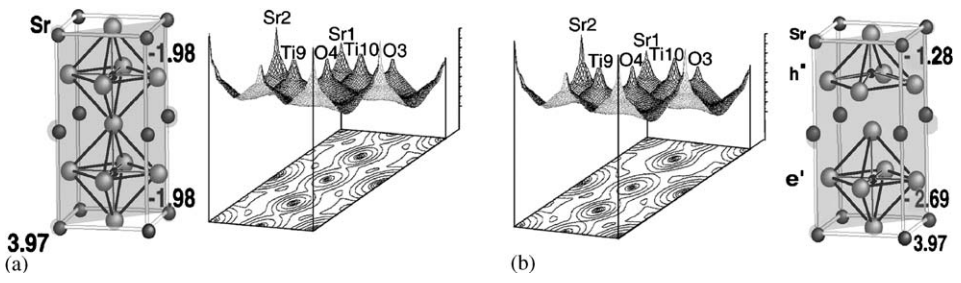

Fig. 8. Density of charge contour and surface plots in a vertical diagonal plane cutting Ti9 and Ti10 for ST-c (left) and ST-a (right). The numbers indicated on the cell representations correspond to the Mulliken net charges for ST-c (left) where $Q_{Sr} = 3.97$ and $Q[TiO_6] = -1.98$ and for ST-a (right) where $Q_{Sr} = 3.97$, $Q[TiO_6] = -2.69$ and $Q[TiO_5] = -1.28$.

charge remains the same, 3.97*e*. A permanent charge gradient is thus created between [TiO_6] and [TiO_5] to compensate the breaking of Ti10–O4 bond. However, the net atomic charges of Ti and O centeres individually suffer few changes: Ti9 gains 0.26*e*, Ti10 0.11*e*, O4 −0.28*e* and the others O less than −0.1*e*. Therefore, the 1e negative charge transfer occurs from one cluster to another and not from the oxygen atom to one titanium atom, following the common idea. This simple net charge calculation from Mulliken analysis allows to identify the hole and electron polarons expected in perovskite-type titanates [48], however, they are not localized on O and Ti atoms like Stashans et al. announced, but on cluster entities. Those polarons, are the trapped hole and electrons that favor the radiative emission process leading to PL. The striking fact is that the trapped holes and electrons that exist in the structurally defective compound are prior to the excitation as our calculation is strictly a ground state calculation. The amorphous thin films already intrinsically possess the necessary condition for creating PL. Moreover, it has to be emphasized that PL does not depend on the temperature but only on the crystalline structure of the material.

6. Conclusions

Thin films of $SrTiO_3$ have been synthesized following a soft chemical processing. They were structurally characterized by means of XRD. Two thin films are more particularly studied in this paper, one crystalline heat treated 973 K for 2 h and one amorphous heat treated at 573 K for 12 h. The corresponding PL properties have been measured and only the amorphous thin film presents the property. To understand the mechanism of this PL behavior in amorphous $SrTiO_3$, we turned to first-principles theory as an appropriate tool of rationalization. Therefore, we have performed DFT calculations on two models that stand for the crystalline and amorphous $SrTiO_3$ films. The theoretical results are confronted with experimental data and both are coherent. The theoretical results indicate that the formation of a fivefold oxygen titanium coordination [TiO_5] through the displacement of Ti10 and the rupture of the Ti10–O4 bond introduces localized electronic levels with O4 ($2p_x$, $2p_y$, $2p_z$) character above the VB of the structure before deformation. The presence of those trapped holes and electrons, existing before the excitation, is the main factor allowing that the radiative emission process strongly prevails on the non-radiative recombination process, and thus that amorphous ST thin film presents strong visible PL at room temperature.

Acknowledgments

This work was partially supported by the Brazilian research-financing institutions: Fundação de Amparo à Pesquisa do Estado de São Paulo-FAPESP/CEPID and Conselho Nacional de Desenvolvimento Científico e Tecnológico-CNPq/PRONEX.

References

[1] R. Leonelli, J.L. Brebner, Solid State Commun. 54 (1985) 505.
[2] L.T. Canham, Appl. Phys. Lett. 57 (1990) 1046.
[3] J. Meng, Y. Huang, W. Zhang, Z. Du, Z. Zhu, G. Zou, Phys. Lett. A 205 (1995) 72.
[4] H. Rinnert, M. Vergat, G. Marchal, A. Burneau, Appl. Phys. Lett. 72 (1998) 3157.
[5] J.F. Scott, Ferroelectrics Rev. 1 (1998) 1.
[6] A.J. Millis, Nature 392 (1998) 147.
[7] B.W. Wessels, Annu. Rev. Mater. Sci. 25 (1995) 525.
[8] M. Cardona, Phys. Rev. A 140 (1965) 651.
[9] M.I. Cohen, R.F. Blunt, Phys. Rev. 168 (1968) 929.
[10] M. Capizzi, A. Frova, Phys. Rev. Lett. 25 (1970) 1298.
[11] K.W. Blazey, Phys. Rev. Lett. 27 (1971) 146.
[12] J.A. Noland, Phys. Rev. 94 (1954) 724.
[13] R. Leonelli, J.L. Brebner, Phys. Rev. B. 33 (12) (1986) 8649.
[14] L. Grabner, Phys. Rev. 177 (1969) 1315.
[15] Y.T. Sihvonen, J. Appl. Phys. 38 (1967) 4431.
[16] W.F. Zhang, Q. Xing, Y.B. Huang, Mod. Phys. Lett. B 14 (19) (2000) 709.
[17] L.E.B. Soledade, E. Longo, E.R. Leite, F.M. Pontes, F. Lanciotti Jr., C.E.M. Campos, P.S. Pizani, J.A. Varela, Appl. Phys. A 75 (5) (2002) 629.
[18] J.H. Rangel, N.L.V. Carreño, E.R. Leite, E. Longo, C.E.M. Campos, F. Lanciotti Jr., P.S. Pizani, J.A. Varela, J. Lumin. 99 (1) (2002) 7.
[19] P.S. Pizani, H.C. Basso, F. Lanciotti, T.M. Boschi, F.M. Pontes, E. Longo, E.R. Leite, Appl. Phys. Lett. 81 (2) (2002) 253.
[20] F. Lanciotti, P.S. Pizani, C.E.M. Campos, E.R. Leite, L.P.S. Santos, N.L.V. Carreño, E. Longo, Appl. Phys. A 74 (6) (2002) 787.
[21] E.R. Leite, F.M.L. Pontes, E.J.H. Lee, R. Aguiar, E. Longo, D.S.L. Pontes, M.S.J. Nunes, H.R. Macedo, P.S. Pizani, F. Lanciotti Jr., T.M. Boschi, J.A. Varela, C.A. Paskocimas, Appl. Phys. A 74 (4) (2002) 529.
[22] E.R. Leite, L.P.S. Santos, N.L.V. Carreño, C.A. Paskocimas, F. Lanciotti Jr., P.S. Pizani, C.E.M. Campos, J.A. Varela, E. Longo, Appl. Phys. Lett. 78 (15) (2001) 2148.
[23] E.R. Leite, F.M.L. Pontes, E.C. Paris, C.A. Paskocimas, E.J.H. Lee, E. Longo, P.S. Pizani, J.A. Varela, V. Mastelaro, Adv. Mater. Opt. Electron. 10 (6) (2000) 235.
[24] F.M. Pontes, E.R. Leite, E. Longo, J.A. Varela, P.S. Pizani, C.E.M. Campos, F. Lanciotti Jr., Adv. Mater. Opt. Electron. 10 (2) (2000) 81.
[25] P.S. Pizani, E.R. Leite, F.M. Pontes, E.C. Paris, J.H. Rangel, E.J.H. Lee, E. Longo, P. Delega, J.A. Varela, Appl. Phys. Lett. 77 (6) (2000) 824.
[26] R.I. Eglitis, E.A. Kotomim, G. Borstel, Eur. Phys. J. B 27 (2002) 483.
[27] B. Bouma, G. Blasse, J. Phys. Chem. Solids 56 (2) (1995) 261.
[28] C.D. Pinheiro, E. Longo, E.R. Leite, F.M. Pontes, R. Magnani, J.A. Varela, P.S. Pizani, T.M. Boschi, F. Lanciotti, Appl. Phys. A 77 (1) (2003) 81.
[29] F.M. Pontes, C.D. Pinheiro, E. Longo, E.R. Leite, S.R. De Lazaro, R. Magnani, P.S. Pizani, T.M. Boschi, F. Lanciotti Jr., J. Lumin. 104 (3) (2003) 175.

[30] E.R. Leite, E.C. Paris, F.M. Pontes, C.A. Paskocimas, E. Longo, C.D. Pinheiro, J.A. Varela, P.S. Pizani, C.E.M. Campos, F. Lanciotti Jr., J. Mater. Sci. 38 (6) (2003) 1775.
[31] F.M. Pontes, C.D. Pinheiro, E. Longo, E.R. Leite, S.R. De Lazaro, J.A. Varela, P.S. Pizani, T.M. Boschi, F. Lanciotti Jr., Mater. Chem. Phys. 78 (1) (2003) 227.
[32] F.M. Pontes, E. Longo, E.R. Leite, E.J.H. Lee, J.A. Varela, P.S. Pizani, C.E.M. Campos, F. Lanciotti Jr., V. Mastellaro, C.D. Pinheiro, Mat. Chem. Phys. 77 (2) (2003) 598.
[33] E. Canadell, P. Ordejón, E. Artacho, D. Sánchez-Portal, A. García, J.M. Soler, J. Mater. Chem. 11 (2001) 1.
[34] R. Hoffmann, Solids and Surfaces, VCH, New York, 1988.
[35] J.K. Burdett, Chemical Bonding in Solids, Oxford University Press, New York, 1995.
[36] E. Canadell, M.H. Whangbo, Chem. Rev. 91 (1991) 965.
[37] F.C.D. Lemos, E. Longo, E.R. Leite, D.M.A. Melo, A.O. Silva, J. Solid State Chem. 177 (2004) 1542.
[38] V.R. Saunders, R. Dovesi, C. Roetti, M. Causa, N.M. Harrison, R. Orlando, C.M. Zicovich-Wilson, CRYSTAL98 User's Manual, University of Torino, Torino, 1998.
[39] C. Lee, W. Yang, R.G. Parr, Phys. Rev. B 37 (1988) 785.
[40] A.D. Becke, J. Chem. Phys. 98 (1993) 5648.
[41] J. Muscat, A. Wander, N.M. Harrison, Chem. Phys. Lett. 42 (2001) 397.
[42] http://www.tcm.phy.cam.ac.uk/~mdt26/crystal.html.
[43] http://www.chimifm.unito.it/teorica/crystal/crystal.html.
[44] A. Kojalj, J. Mol. Graph. Model. 17 (1999) 176.
[45] L.G.J. de Haart, A.J. de Vries, G. Blasse, J. Solid State Chem. 59 (1985) 291.
[46] J.S. Zhu, X.M. Lu, W. Jiang, W. Tian, M. Zhu, M.S. Zhang, X.B. Chen, X. Liu, Y.N. Wang, J. Appl. Phys. 81 (3) (1997) 1392.
[47] G. Blasse, B.C. Grabmaier, Luminescent Materials, Springer, Berlin, Heildelberg, 1994.
[48] A. Stashans, H. Pinto, P. Sanchez, J. Low Temp. Phys. 130 (3/4) (2003) 415.